



APPLICATION OF EXTENDED KALMAN FILTER IN ESTIMATION OF REENTRY TRAJECTORIES

Guilherme da Silveira

IAE – Instituto de Aeronáutica e Espaço
Praça Mal. Eduardo Gomes, 50
12228904 – São José dos Campos, SP – BRAZIL
guilhermegs@iae.cta.br

Helio Koiti Kuga

INPE – Instituto Nacional de Pesquisas Espaciais
Av. dos Astronautas, 1758
12227010 – São José dos Campos, SP – BRAZIL
hkk@dem.inpe.br

Élcio Jerônimo de Oliveira

IAE – Instituto de Aeronáutica e Espaço
Praça Mal. Eduardo Gomes, 50
12228904 – São José dos Campos, SP – BRAZIL
elcioejo@iae.cta.br

Abstract. Atmospheric reentry dynamics of space vehicles represents a complex phenomenon for which a mathematical model is difficult to obtain, partly because of the uncertainty related to the aerodynamic efforts acting on the vehicle during reentry. The use of estimation techniques to determine the unknown parameters of the vehicle dynamics can help to enlighten this phenomenon. This work presents the data processing of the atmospheric reentry of the platform Plataforma SubOrbital (PSO1), a microgravity platform launched from the Centro de Lançamento da Barreira do Inferno (CLBI), in Natal, Brazil, in 2000. Using actual flight position data, relative to CLBI's radar, and applying an Extended Kalman Filter methodology, the variables that describe the dynamic behavior of the platform are estimated. The mathematical model of the platform during reentry is composed of five state variables: two positions, two velocities and one aerodynamic parameter. The aerodynamic efforts acting on the platform depend to great extent on such parameter. Results have shown correct position estimation, reflected in low filter residues, and consistent velocity estimation. The aerodynamic parameter grows after the platform reenters the atmosphere, and its value depends on the dynamic noise level associated with the dynamic model. The values of the standard deviation associated with the state vector are considered in both the filter tuning and convergence analysis, showing consistency of the aerodynamic characteristics.

Keywords: Extended Kalman filter, reentry trajectories, estimation

1. INTRODUCTION

The platform PSO1 (Milani, 1995) is a suborbital platform, developed at the Instituto Nacional de Pesquisas Espaciais – INPE –, Brazil, employed to perform experiments on an environment of microgravity, environment which is created when the platform experiences a free-fall trajectory in vacuum. To achieve this situation, the platform is launched with the aid of a sounding rocket, experiences an acceleration until the burn out of the rocket and then follows an approximately parabolic trajectory, reaching a maximum altitude outside the Earth atmosphere and then reenters the atmosphere. Usually, the microgravity environment is considered to occur during the time span the platform is above 100 km altitude, when the aerodynamic efforts acting on it are negligible.

During the atmospheric reentry, the aerodynamic efforts acting on the platform become more important as the atmospheric density grows from a nearly zero value to its value at sea level. A good prediction of the platform's trajectory during reentry must take into consideration these efforts.

A launch mission of PSO1 occurred in 2000, using the sounding rocket Sonda III to launch the platform. This mission allowed the acquisition of position data of the platform during its reentry trajectory, in terms of azimuth, elevation and distance relative to the radar which performed the measurements. Using an Extended Kalman filter, this work presents an estimation of the reentry trajectory of PSO1 for this mission. Position and velocity are estimated, as well as the aerodynamic drag acting on the platform.

The problem of reentry trajectory estimation was addressed in works of Austin and Leondes (1981), Julier and Uhlmann (2004a), Julier and Uhlmann (2004b) and Milani, *et al.* (2012). Specifically, Milani, *et al.*, (2012) has analyzed the same data of PSO1 presented here, but using a different filtering approach.

2. THE EXTENDED KALMAN FILTER

The extended Kalman filter is an estimation algorithm designed to deal with non linear systems dynamics (Maybeck, 1979; Brown and Hwang, 1992). In this work it is considered a system and observation dynamics in the continuous-discrete form presented in Eq. (1) and (2), where \mathbf{x} is the state vector of the system, \mathbf{y} is the system output, \mathbf{f} and \mathbf{h} are non-linear vector equations, G is a noise input matrix and \mathbf{w} and \mathbf{v} are the dynamic and measurement vector noises, assumed to be zero-mean independent Gaussian distributions. The subscript k indicates the time instant t_k .

$$\dot{\mathbf{x}}(t) = \mathbf{f}(\mathbf{x}, t) + G(t)\mathbf{w}(t) \quad (1)$$

$$\mathbf{y}_k = \mathbf{h}_k(\mathbf{x}_k) + \mathbf{v}_k \quad (2)$$

The filter algorithm consists of two phases of data processing: time update (prediction) and measurement update (correction) (Maybeck, 1979; Kuga, 2005). During prediction phase, the state of the system, as well as its covariance matrix, is propagated in time. The initial condition for this propagation is the estimated value of the state and covariance from the previous filter step. During correction phase, using the available measurements of the system output at that time instant, the state and covariance of the system are updated. Propagated values (values of estate and covariance before the correction phase) at t_k are indicated by $\bar{\mathbf{x}}_k$ and \bar{P}_k ; corrected values (values of state and covariance after the correction phase) are indicated by $\hat{\mathbf{x}}_k$ and \hat{P}_k .

The prediction phase from time t_{k-1} to t_k can be calculated with Eq. (3) and (4), resulting in the predicted values $\bar{\mathbf{x}}_k$ and \bar{P}_k , where F is the Jacobian matrix of the dynamic model given by Eq. (5). The initial conditions for the propagation are the estimated values from the previous filter step: $\bar{\mathbf{x}}(t_{k-1}) = \hat{\mathbf{x}}_{k-1}$ and $\bar{P}(t_{k-1}) = \hat{P}_{k-1}$.

$$\dot{\bar{\mathbf{x}}}(t) = \mathbf{f}(\bar{\mathbf{x}}, t) \quad (3)$$

$$\dot{\bar{P}}(t) = F(t)\bar{P}(t) + \bar{P}(t)F(t)^T + G(t)Q(t)G(t)^T \quad (4)$$

$$F = \left[\frac{\partial \mathbf{f}}{\partial \mathbf{x}} \right] \quad (5)$$

The correction phase incorporates the measurements at time t_k , resulting in the estimated values of the state and covariance, as presented in Eq. (6) to (8), where H_k is the Jacobian matrix of the observation model, given by Eq. (9).

$$K_k = \bar{P}_k H_k^T (H_k \bar{P}_k H_k^T + R_k)^{-1} \quad (6)$$

$$\hat{P}_k = (I - K_k H_k) \bar{P}_k \quad (7)$$

$$\hat{\mathbf{x}}_k = \bar{\mathbf{x}}_k + K_k [\mathbf{y}_k - \mathbf{h}_k(\bar{\mathbf{x}}_k)] \quad (8)$$

$$H_k = \left[\frac{\partial \mathbf{h}_k}{\partial \mathbf{x}} \right]_{\mathbf{x}=\bar{\mathbf{x}}_k} \quad (9)$$

A measure of the state estimation uncertainty is given by the covariance or the standard deviation associated with the state, where the standard deviation is the root square of the diagonal elements of the covariance matrix.

3. ATMOSPHERIC REENTRY DYNAMICS

The system dynamic model adopted in this work follows from (Milani, *et al.*, 2012). The reentry trajectory of PSO1 is considered to take place in a plane and the model is composed of five state variables: two variables describing the horizontal and vertical positions (x_1 and x_2 , respectively) and another two describing horizontal and vertical velocities

(x_3 and x_4 , respectively); one last variable estimates the aerodynamic effort acting on the platform (x_5). An inertial coordinate frame is considered to have its origin on the center of the Earth, with one axis passing through the radar point on the surface – vertical axis – and another axis lying on the plane of the trajectory – horizontal axis –, as shown in Fig. 1.

Two forces act on the platform during reentry. The first type is the gravitational force, which accelerates the platform toward the Earth center. The second type is the aerodynamic force, which depends on atmospheric density and vehicle speed. In this work, only an aerodynamic drag was considered, resulting in a force always opposed to the vehicle velocity vector.

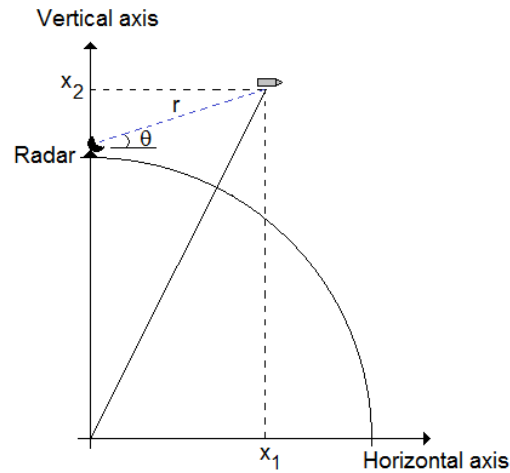


Figure 1. Reentry geometry

The platform state equations are shown in Eq. (10), where G_k is the term related to the gravitational force, D_k is the term related to the drag force and $w_{i,k}$ is the dynamic noise vector. The force terms are given by Eq. (11) to (13), where $R_k = \sqrt{x_{1,k}^2 + x_{2,k}^2}$ is the distance from Earth center to the platform and $V_k = \sqrt{x_{3,k}^2 + x_{4,k}^2}$ is the platform speed. The values $\beta_0 = -0.59783 \text{ km}^{-1}$, $H_0 = 13.406 \text{ km}$, $GM = 3.9860 \times 10^5 \text{ km}^3 \text{ s}^{-2}$ and $R_0 = 6374 \text{ km}$ reflect typical environmental and vehicle characteristics (Julier and Uhlmann, 2004a).

$$\begin{aligned}\dot{x}_{1,k} &= x_{3,k} \\ \dot{x}_{2,k} &= x_{4,k} \\ \dot{x}_{3,k} &= G_k x_{1,k} + D_k x_{3,k} + w_{1,k} \\ \dot{x}_{4,k} &= G_k x_{2,k} + D_k x_{4,k} + w_{2,k} \\ \dot{x}_{5,k} &= w_{3,k}\end{aligned}\quad (10)$$

$$D_k = \beta_k \exp\left\{\frac{R_0 - R_k}{H_0}\right\} V_k \quad (11)$$

$$G_k = -\frac{GM}{R_k^3} \quad (12)$$

$$\beta_k = \beta_0 \exp\{x_{5,k}\} \quad (13)$$

The position of the vehicle is measured relative to a tracking station located at $(0, R_0)$. The tracking station measures the distance, r_k , and elevation, θ_k , so that the observation model is described by Eq. (14) and (15), where $v_{i,k}$ is the measurement noise vector.

$$r_k = \sqrt{x_{1,k}^2 + (x_{2,k} - R_0)^2} + v_{1,k} \quad (14)$$

$$\theta_k = \tan^{-1} \left(\frac{x_{2,k} - R_0}{x_{1,k}} \right) + v_{2,k} \quad (15)$$

4. PSO1 MISSION DATA AND SETUP

The measured data of the trajectory of PSO1 consist of azimuth, elevation and distance from the tracking station. As in this work the trajectory is considered to take place in a plane, only elevation and distance need to be taken into consideration. Using this information, the position of the platform relative to the center of the Earth was calculated. The analysis presented here has as initial time the apogee of the actual trajectory of PSO1, to which was attributed $t_0 = 0$ s. At this instant, the vehicle is considered to have only horizontal velocity. The measured reentry trajectory of PSO1 is presented in Fig. 2, where the cross indicates the radar position on the surface of the Earth.

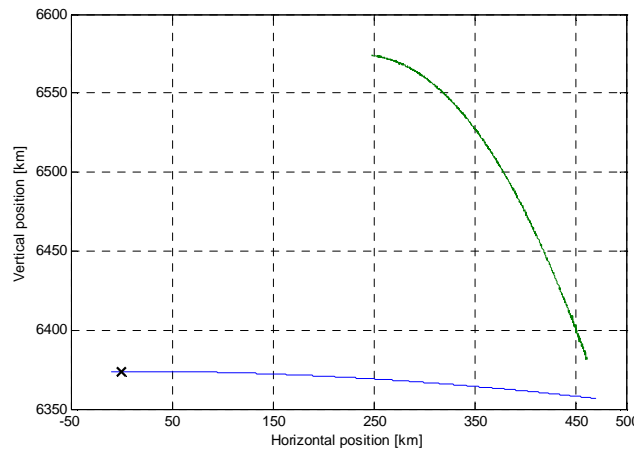


Figure 2. Measured reentry trajectory of PSO1

The initial conditions of the state for the application of the filter algorithm are

$$\hat{\mathbf{x}}_0 = (248.0 \text{ km} \quad R_0 + 199.6 \text{ km} \quad 1.1 \text{ km/s} \quad 0 \text{ km/s} \quad 0)^T.$$

The initial condition for the covariance matrix is a diagonal matrix whose diagonal elements are all equal to 10^{-5} :

$$\hat{P}_0 = \text{diag} [10^{-5} \quad 10^{-5} \quad 10^{-5} \quad 10^{-5} \quad 10^{-5}].$$

Different values of dynamic noise were used to tune the filter. The tuned values will be presented in the next section, along with the corresponding filter results. The dynamic noise covariance matrix is denoted by

$$Q = \text{diag} [q_1 \quad q_2 \quad q_3].$$

Considering that the dynamic noise is associated only with state variables x_3 , x_4 and x_5 , and that there is no coupling effects, the G matrix is chosen so that the dynamic noise term in Eq. (4) is given by

$$GQG^T = \text{diag} [0 \quad 0 \quad q_1 \quad q_2 \quad q_3].$$

Concerning the measurement noise, the adopted standard deviation in distance is of 10 m and in elevation is of 1.7×10^{-3} rad, resulting in the following covariance matrix:

$$R = \text{diag} [10^{-4} \quad 3 \times 10^{-6}].$$

5. RESULTS

As a first attempt to tune the filter, the following covariance matrix for the dynamic noise was adopted (Julier and Uhlmann, 2004a):

$$Q = \text{diag} \left[2.4 \times 10^{-5} \quad 2.4 \times 10^{-5} \quad 10^{-6} \right].$$

The measured and estimated position are presented in Fig. 3. It can be seen a good agreement between them during almost all reentry flight. At the end of the trajectory, due to low elevation values, the filter has more difficulty to estimate the position. This fact is apparent when analyzing the residues in distance and elevation, shown in Fig. 4a. After an expected transient at the beginning, the residues remain oscillating close to zero and augment at the end of the estimation process. To verify the hypothesis of a zero-mean Gaussian dynamic noise, Fig. 4b shows a histogram of the residues for the central portion of Fig. 4a – from 4.55 to 160.00 s.

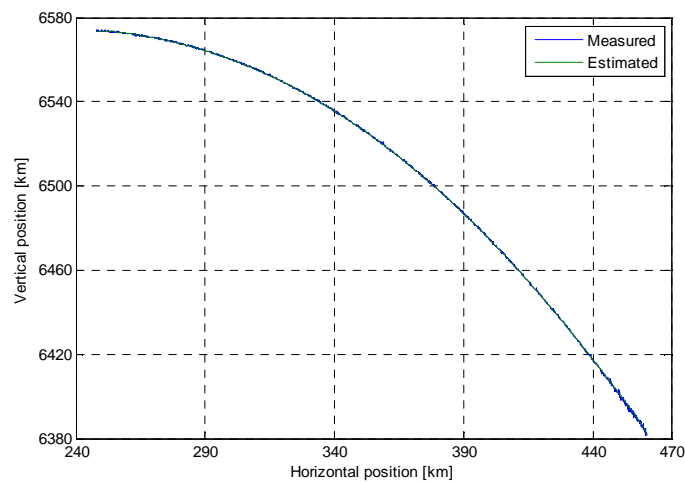


Figure 3. Measured and estimated trajectory using $Q = \text{diag} \left[2.4 \times 10^{-5} \quad 2.4 \times 10^{-5} \quad 10^{-6} \right]$

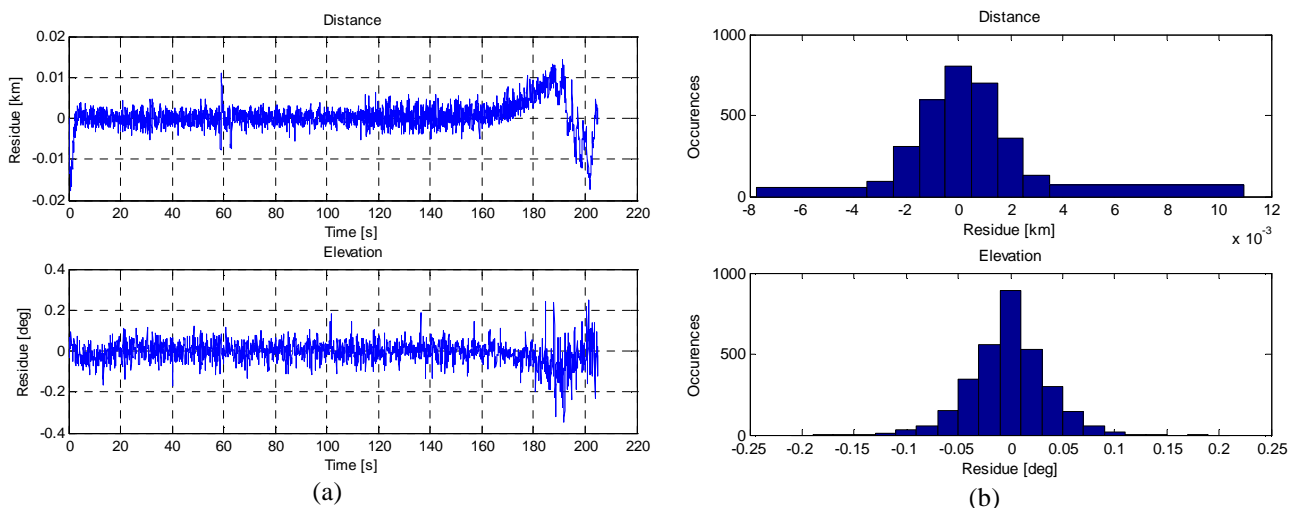


Figure 4. (a) Filter residues and (b) residues histogram using $Q = \text{diag} \left[2.4 \times 10^{-5} \quad 2.4 \times 10^{-5} \quad 10^{-6} \right]$

The estimated velocity of the platform and the estimated aerodynamic parameter are shown in Fig. 5, along with the respective standard deviation. The horizontal velocity remains almost constant during the exoatmospheric trajectory and, as the atmospheric density grows and the drag force becomes more important, its value decreases. The vertical velocity grows from zero at trajectory's apogee, reaches a maximum value, and then decreases as the aerodynamic drag becomes more important. The standard deviations associated with these states remain small compared to the value of the states. The aerodynamic parameter x_5 begins to change for an altitude of approximately 60 km. It grows to high

Guilherme da Silveira, Helio Koiti Kuga and Elcio Jeronimo Oliveira
Application of Extended Kalman Filter in Estimation of Reentry Trajectories

values characterizing the high atmospheric friction at high vertical velocities. Then it starts to decrease as the parachute is opened and the velocity decreases as well. It is important to remark that these timewise variations of the aerodynamic coefficient could be estimated in the sequential Kalman filter implementation and with enough data providing observability to the system. The standard deviation associated with this state is relatively large, resulting in a large uncertainty of this parameter.

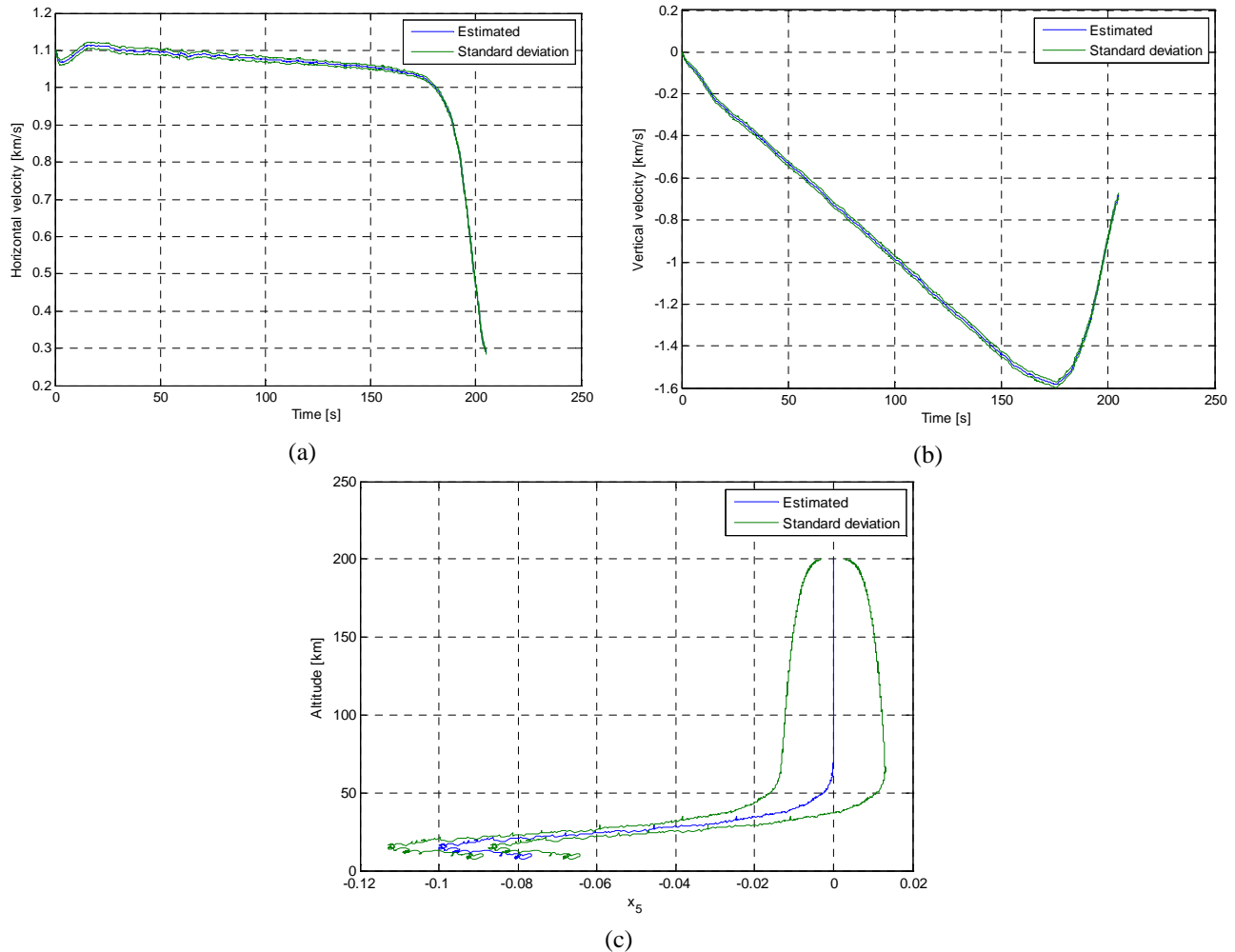


Figure 5. (a) Estimated horizontal velocity; (b) estimated vertical velocity and (c) estimated aerodynamic parameter using $Q = \text{diag} [2.4 \times 10^{-5} \quad 2.4 \times 10^{-5} \quad 10^{-6}]$

In order to test the filter sensibility to the tuning parameters, other values of filter noises were considered. A first essay was to consider the noise associated with the horizontal acceleration ten times bigger than the one associated with the vertical acceleration, since the horizontal range is considerably smaller and, therefore, is more influenced by model errors than the vertical range. The following constant covariance matrix for the dynamic noise was adopted

$$Q = \text{diag} [2.4 \times 10^{-4} \quad 2.4 \times 10^{-5} \quad 10^{-6}].$$

The comparison of residues for the two considered cases is shown in Fig. 6. It can be seen an improvement in the residue associated with the distance at the end of filtering process. On the other hand, the estimated horizontal velocity becomes noisier, as can be seen in Fig. 7a, and the standard deviation associated with it becomes bigger, as can be seen in Fig. 7b. The difference in the aerodynamic parameter is shown in Fig. 8. No significant difference on the standard deviation was observed for this state.

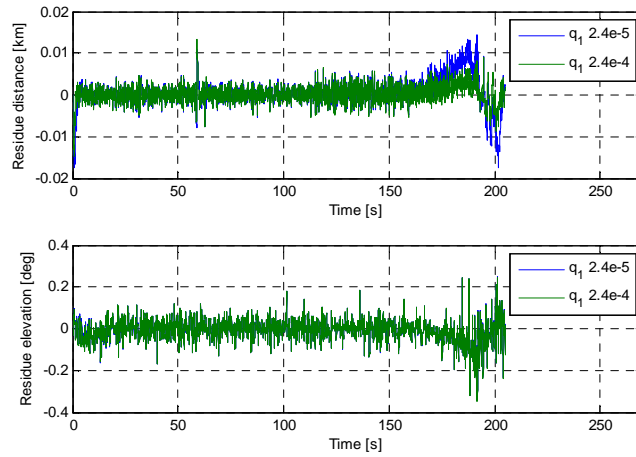


Figure 6. Filter residues comparison for $q_1 = 2.4 \times 10^{-5}$ and $q_1 = 2.4 \times 10^{-4}$

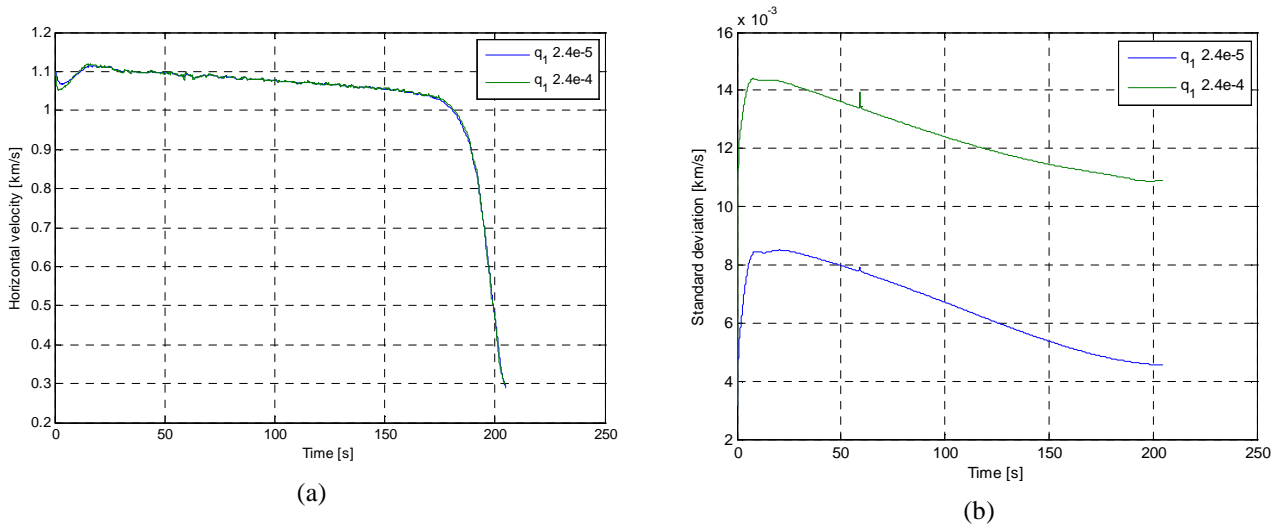


Figure 7. (a) Estimated horizontal velocity and (b) horizontal velocity standard deviation comparison for $q_1 = 2.4 \times 10^{-5}$ and $q_1 = 2.4 \times 10^{-4}$

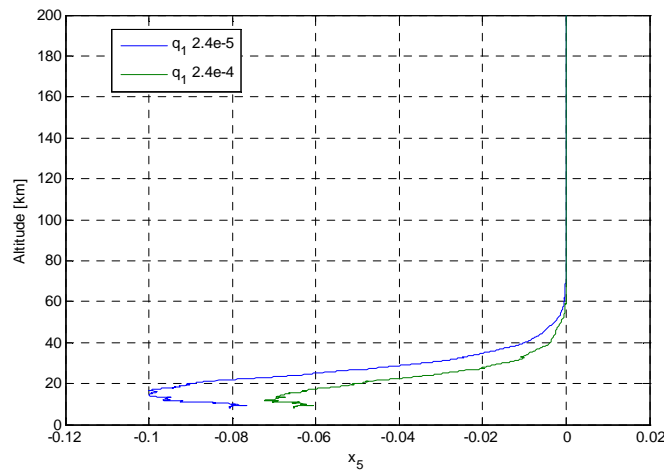


Figure 8. Estimated aerodynamic parameter comparison for $q_1 = 2.4 \times 10^{-5}$ and $q_1 = 2.4 \times 10^{-4}$

The influence of the dynamic noise associated with the aerodynamic parameter on the filter behavior was also investigated. Reducing the values of q_3 from 10^{-6} to 10^{-8} , in spite of affecting the aerodynamic parameter itself, does not affect considerably other results like the estimated velocity and residues. On the other hand, if the noise is augmented to $q_3 = 10^{-4}$, there is a change on the results, as can be seen on Fig. 9 and 10. There is an improvement on the filter residues both for distance and elevation. Figure 11 shows, however, that the use of this value for q_3 causes the standard deviation to have an abrupt augmentation at the end of the estimation process for the velocity components, a behavior not expected for the filter. The standard deviation associated with the aerodynamic parameter also augments, but it keeps the same relation with the estimated value of this parameter presented for the previous cases.

Such behavior of the filter shows clearly the existing coupling between the aerodynamics drag and velocity error estimates. At this point, because the obtained residues are equivalent, there is no definition of which of the dynamic noise values worked better. One can point out that the dynamic noise corresponding to the aerodynamic parameter should be somewhere between 10^{-6} and 10^{-4} . This shows clearly the difficulty in tuning the filter to obtain consistent results.

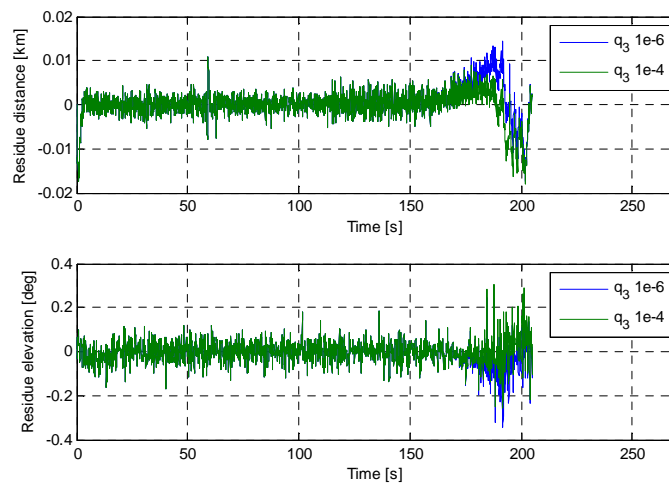


Figure 9. Filter residues comparison for $q_3 = 1 \times 10^{-6}$ and $q_3 = 1 \times 10^{-4}$

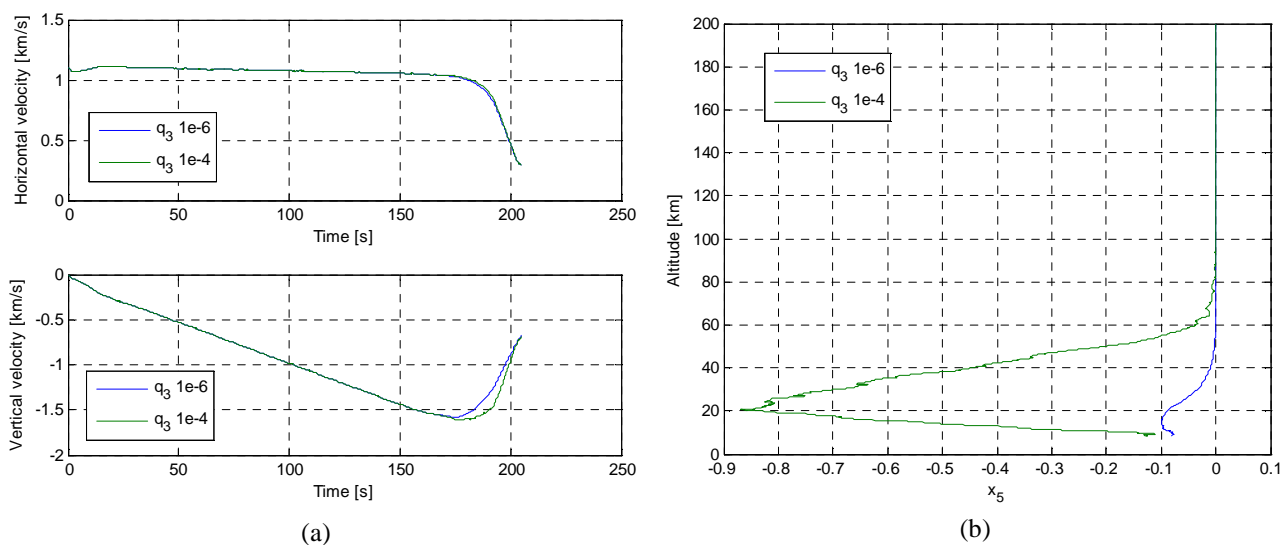


Figure 10. (a) Estimated velocity and (b) estimated aerodynamic parameter comparison for $q_3 = 1 \times 10^{-6}$ and $q_3 = 1 \times 10^{-4}$

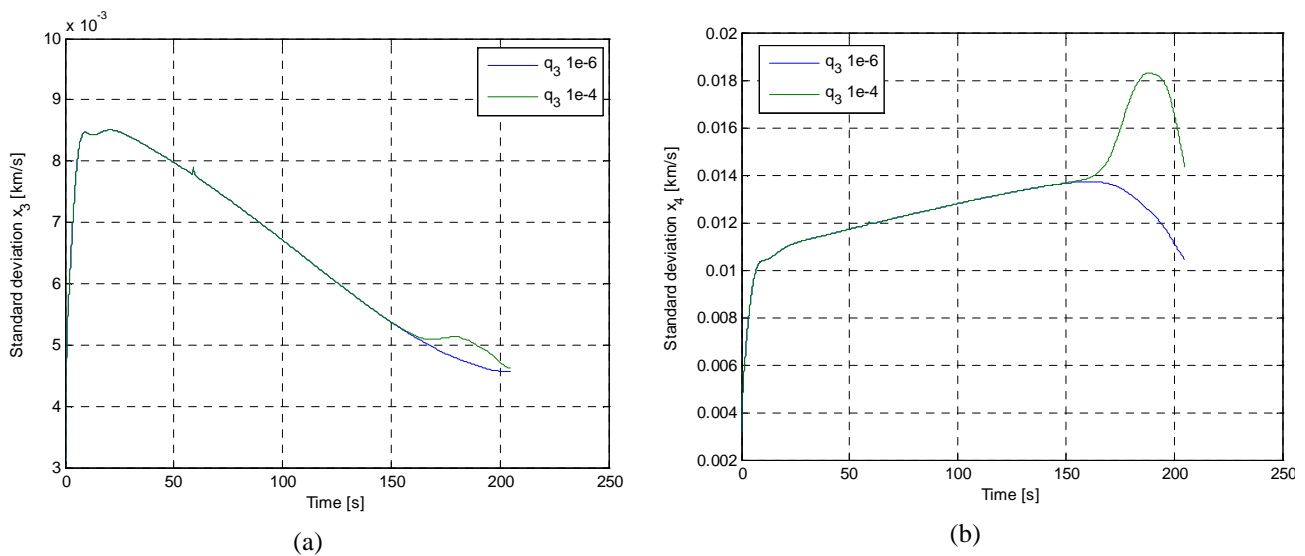


Figure 11. (a) x_3 standard deviation and (b) x_4 standard deviation comparison for $q_3 = 1 \times 10^{-6}$ and $q_3 = 1 \times 10^{-4}$

6. CONCLUSIONS

This work presented the application of the Extended Kalman filter to the reentry problem of a suborbital platform. From the actual measured data of distance and elevation related to the radar location, the position and velocity of the platform were estimated, as well as an aerodynamic parameter which describes the aerodynamic effort acting on the platform during reentry. The methodology provided good results for the position estimation, resulting in low filter residues. The estimated velocity is coherent with the velocity of a reentry object, providing a means of determining the velocity of such an object when only position data are available, as was the case of PSO1 mission. The estimated states depend on the adopted dynamic noise. This fact is more apparent for the aerodynamic parameter. Although there was a high variation of this estimated parameter with several levels of noise, its impact on the other estimated states – position and velocity – was relatively small. The uncertainty related with the estimated parameters, in the form of the standard deviation, indicates that the dynamic model could be improved to better estimate the aerodynamic parameter. Consideration of a three dimensional dynamics and aerodynamic lift force could be implemented to try to improve the results.

A recommended future work is to estimate the aerodynamic parameter with a first order Gauss-Markov approach (Oliveira, *et al.*, 2009) as well as an adaptive scheme to evaluate the dynamical noise timewise (Kuga, 1982; Jazwinski, 1969).

7. REFERENCES

- Austin, J.W. and Leondes, C.T., 1981. "Statistically linearized estimation of reentry trajectories". *Aerospace and Electronic Systems*, Vol. 17, p. 54-61.
- Brown, R.G. and Hwang, P.Y.C., 1992. *Introduction to Random Signals and Applied Kalman Filtering, Second Edition*. John Wiley & Sons, Inc, New York.
- Jazwinski, A.H., 1969. "Adaptive Filtering". *Automatica*, Vol. 5, p. 475-485.
- Julier, S.J. and Uhlmann, J.K., 2004a. "Unscented filtering and nonlinear estimation". *Proceedings of the IEEE*, Vol. 92, p. 401-422.
- Julier, S.J. and Uhlmann, J.K., 2004b. "Corrections to unscented filtering and nonlinear estimation". *Proceedings of the IEEE*, Vol. 92, p. 1958.
- Kuga, H.K., 1982. *Estimação adaptativa de órbitas aplicada a satélites a baixa altitude*. Master thesis, Instituto Nacional de Pesquisas Espaciais, São José dos Campos.
- Kuga, H.K., 2005. *Noções práticas de técnicas de estimação*. Class notes, Instituto Nacional de Pesquisas Espaciais, São José dos Campos.
- Maybeck, P.S., 1979. *Stochastic Models, Estimation, and Control – Volume 1*. Academic Press, New York.
- Milani, P.G., 1995. "Os Experimentos Tecnológicos da Plataforma SubOrbital - PSO1". In *I Simposio Brasileiro de Engenharia Inercial*, Vol. 1.
- Milani, P.G., Bambace, L.A.W. and Guedes, U.T.V., 2012. "Sobre o uso de um filtro de Kalman unscented para o processamento de dados reais de voo de veículo em uma reentrada atmosférica". In *Proceedings of VII SBEIN - Simpósio Brasileiro de Engenharia Inercial*. São José dos Campos, Brazil.

Guilherme da Silveira, Helio Koiti Kuga and Elcio Jeronimo Oliveira
Application of Extended Kalman Filter in Estimation of Reentry Trajectories

Oliveira, E.J., Kuga, H.K. and Lopes, R.V.F., 2009. "IMU self-alignment on a static platform with Kalman filter". In *Proceedings of 8th Brazilian Conference on Dynamics, Control and Applications*, p. 1-6.

8. RESPONSIBILITY NOTICE

The authors are the only responsible for the printed material included in this paper.